Optimal Power Dispatch for a Chlorine Factory With Fuel Cells Participating in Incentive-Based Demand Response

Leehter Yao, *Senior Member, IEEE*, and Jin Chuan Teo

***Abstract*—A system integrating fuel cells with the power system of a chlorine factory that produces hydrogen as a byproduct during chlorine production is proposed. In order to maximize the factory's profit, in this article, a comprehensive optimal power dispatch algorithm (COPDA) is designed in the factory's energy management system. In the proposed COPDA, the power consumption of the factory's electrolyzer, the output power of fuel cells, and the power purchased from the grid are optimized. Furthermore, mixed-integer linear programming (MILP) is utilized as the optimization scheme for COPDA. The nonlinearity between the chlorine production rate and the power consumption of the electrolyzer, and between the output power of fuel cells and the hydrogen consumption is solved with a piecewise linearization scheme integrated with the MILP constraints. Profit maximization using COPDA is conducted in the environment of time-varying electricity prices. To further increase profit, the chlorine factory is arranged to participate in an incentive-based demand response program. The COPDA can further maximize the factory's profit for the incentive-based demand response program.**

***Index Terms*—Chlorine factory, demand response (DR), fuel cell (FC), linear programming, power dispatch.**

I. Introduction

ENERGY is the foundation of modern society [1]. Countries depend highly on electricity for their progress and development [2]. The maximum share of the world's electricity generation is based on fossil fuels. However, fossil fuel based power generation induces greenhouse gas (GHG) emissions. In recent years, GHG emissions have caused a significant increase in the global temperature and contributed to climate change [3]. Presently, the threat and rate of climate change are at their peaks [4]. Numerous countries are exerting more effort to implement GHG emission reduction measures, including the adoption of renewable energy sources, curtailment of fossil fuel energy use, and improvements in energy efficiency [5], [6]. Since the power from the grid relies mainly on conventional power plants that use more fossil fuels than other energy resources, using electricity from the grid can contribute to GHG emissions. This is especially obvious in industrial manufacturing and production, which account for the maximum share of power consumption in the energy demand sector. To help mitigate GHG emissions resulting from grid power consumption, factories that produce hydrogen as a byproduct during their production process, such as chlorine factories [7], can reduce their grid power consumption by generating electricity using the byproduct hydrogen through fuel cells (FCs) [8]. This is because the power generated from FC can be appropriately controlled and integrated with the power from the grid to meet the factory's load demand through an energy management system, thereby reducing their grid power consumption. By generating electricity from the byproduct hydrogen, a factory can meet its load demand using the hydrogen-generated electricity, enhancing the factory's flexibility in grid power usage. This, in turn, improves the factory's ability to alternate grid power consumption in response to electricity prices and/or financial incentives offered by the utility company, ultimately enhancing the demand response (DR) potential of these factories.

Numerous power dispatch schemes have been proposed for chlorine factories in the literature. In [9], an optimization model was formulated using mixed-integer nonlinear programming to schedule caustic soda and chlorine production so that the power cost can be minimized under time-varying electricity prices while reducing the peak demand. In [10], a dynamic model dedicated to the power dispatch of chlorine production was developed and used to schedule chlorine production under time-varying electricity prices to minimize the electricity cost. In [11], the Hammerstein–Wiener model parameterization was used to represent the nonlinear process dynamics of chlorine production. Based on the model, a stochastic programming formulation was developed to determine the optimal load allocation for the day-ahead and real-time markets, considering the uncertainty in electricity prices and chlorine demand. A two-stage stochastic programming framework was formulated in [12] to schedule the production of chlorine and byproducts considering the uncertainty in the day-ahead electricity prices. The optimal power dispatch schemes in [13] and [14] allow switching between

Manuscript received 8 December 2022; revised 12 September 2023; accepted 7 October 2023. This work was supported by the Ministry of Science and Technology, Taiwan, under Grant MOST 110-2221-E-027-054-MY3. Paper no. TII-22-5019. *(Corresponding author: Leehter Yao.)*

The authors are with the Department of Electrical Engineering, National Taipei University of Technology, Taipei 10648, Taiwan (e-mail: ltyao@ntut.edu.tw; teojinchuan@gmail.com).

Color versions of one or more figures in this article are available at https://doi.org/10.1109/TII.2023.3326536.

Digital Object Identifier 10.1109/TII.2023.3326536

TABLE I
COMPARISON OF THE PROPOSED COPDA WITH OTHER POWER DISPATCH SCHEMES

Reference	Generate electricity from the by product hydrogen using FC	Consider storage of by product hydrogen	Consider nonlinear relationship between FC power output and hydrogen consumption	Consider nonlinear relationship between EL chlorine production and power consumption	Consider incentive-based DR program
[9]	No	Yes	No	Yes	No
[10], [11], [12]	No	No	No	No	No
[13], [14]	No	No	No	Yes	No
[15], [16]	Yes	No	Yes	Yes	No
[17]	Yes	Yes	No	No	No
Proposed COPDA	Yes	Yes	Yes	Yes	Yes

two operation modes by integrating a chlorine tank to meet the chlorine demand during downtime. Although these optimal power dispatch schemes schedule chlorine production optimally, they do not consider using the byproduct hydrogen for electricity generation but for sale. This does not respond to the concept of reducing grid electricity consumption and, therefore, does not help to mitigate the GHG emissions associated with grid electricity generation.

In [15] and [16], the byproduct hydrogen was utilized for electricity generation to reduce the power purchased from the grid. However, they did not consider storing the byproduct hydrogen. Thus, the use of the byproduct hydrogen is not shiftable, as it is used to generate electricity immediately after it is produced. This approach may potentially arise from a desire to avoid the technological challenges and facility costs associated with hydrogen storage, which have been thoroughly reviewed in [17] and [18] but they are not the focus of this article. The DR potential of chlorine factories can be enhanced if the use of the byproduct hydrogen can be shifted. The power dispatch scheme in [19] considers the storage of the byproduct hydrogen so that its use is controllable and shiftable. However, Teichgraeber and Brandt [19] only considered optimizing the power dispatch of chlorine factories under time-varying electricity prices, without considering incentive-based DR.

The electrolyzer (EL) in a chlorine factory consumes much electricity; usually, more than 90% of a chlorine factory's total electrical load is due to EL load. If a part of the power consumed by EL is generated from an FC using the byproduct hydrogen, the power purchased from the grid can be controlled and managed. The financial profit can be further increased if the chlorine factory participates in the incentive-based DR program under time-varying electricity prices. Moreover, the optimal power dispatch scheme in [19] considered that the hydrogen consumption of the FC varies linearly with the FC output power. This results in a measurement of the FC output power with reduced accuracy, thereby inducing limited the accurate power dispatch results. This is because the output power of the FC varies nonlinearly with hydrogen consumption [20], [21]. Along with chlorine production, the ratio of hydrogen generation to chlorine production is fixed [22].

In this article, a comprehensive optimal power dispatch algorithm (COPDA) is proposed to maximize the profit of a chlorine factory. The difference between the proposed COPDA and the previously published power dispatch scheme is summarized in Table I. As depicted in Table I, the proposed COPDA offers a comprehensive power dispatch strategy tailored to chlorine factories. It optimizes the power dispatch of chlorine factories by collectively considering various important aspects. To the best of our knowledge, the proposed COPDA is the first power dispatch scheme to consider optimizing power dispatch of chlorine factory under an incentive-based DR program. To enable the proposed COPDA to optimize the power dispatch of a chlorine factory under an incentive-based DR program, a novel conditional cost function is developed to calculate the incentive payoff awarded to the factory or the penalty imposed on it, based on the factory's power dispatch decisions made in response to the incentive-based DR program. However, the conditional cost functions are incompatible with mixed-integer linear programming (MILP), resulting in the proposed COPDA being unable to be solved by using readily available MILP solvers. It is always highly recommended to solve the proposed COPDA using the readily available MILP solvers that have been well developed and thoroughly tested by reputable developers for reliability assurance. Therefore, in this article, delicately designed constraints are used to reformulate the conditional cost function into an equivalent form that is compatible with MILP so that the proposed COPDA can be solved by the readily available MILP solvers. To enable the accurate power dispatch, the nonlinear relationships between the FC power output and hydrogen consumption and that between the EL power consumption and chlorine production are considered in the proposed COPDA. However, these nonlinear relationships are incompatible with MILP, preventing the COPDA from being solved by readily available MILP solvers. Piecewise linearization technique is employed with delicately designed constraints to reformulate the nonlinear relationships into an equivalent form that is compatible with MILP so that the COPDA can be solved by readily available MILP solvers. Extensive experiments are designed and conducted to confirm that the MILP-compatible equivalent form of the nonlinear relationship is correctly formulated. Note that, not too many existing works consider nonlinear relationships in both EL and FC, as shown in Table I. Moreover, these works do not undertake the verification process to validate the correctness of the MILP-compatible equivalent form of the nonlinear relationships.

The technical novelties and main contributions of this article are summarized as follows.

1) A system structure integrating FCs in the power system for a chlorine factory or a factory that produces hydrogen as a byproduct in its manufacturing process is proposed.

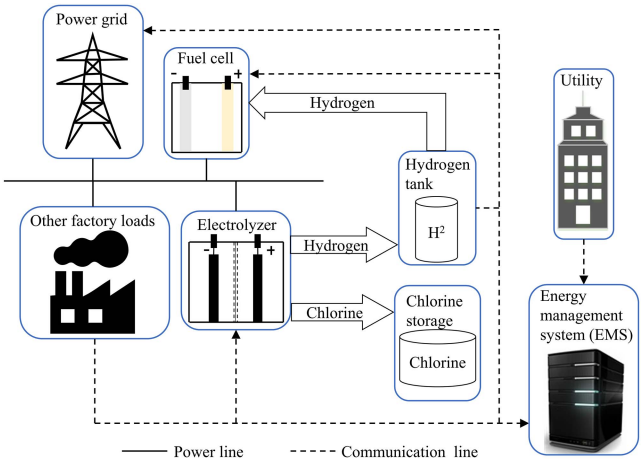

Fig. 1. System structure of the chlorine factory.

2) A comprehensive power dispatch scheme, COPDA, is designed in the energy management system (EMS) to maximize the chlorine factory's profit by maximizing the profits from selling the chlorine and remaining byproduct hydrogen, thus minimizing the cost of power purchased from the grid under time-varying electricity prices and maximizing the incentive payoffs for the incentive-based DR.
3) A piecewise linearization scheme, along with delicate constraints, is designed for MILP so that the nonlinear relationships between the produced chlorine and power consumption and between the FC output power and hydrogen consumption are considered in the optimization of COPDA.
4) A delicate scheme is designed for MILP to solve the conditional cost functions of the incentive payoff or penalty charge to the factory regarding the incentive-based DR.

The rest of this article is organized as follows. Section II describes the chlorine factory. Section III models the chlorine and hydrogen production. Section IV models the electrical power of the factory. Section V describes the FC optimal power dispatch algorithm and the proposed conditional cost function for the DR incentive payoff. Piecewise linear approximations to the nonlinear relationship between hydrogen consumption and FC power output and between chlorine production and EL power consumption are applied in Section VI. The conditional cost function for the DR incentive payoff is reformulated in Section VII. The power dispatch results obtained by the COPDA are presented and evaluated in Section VIII. Finally, Section IX concludes this article.

II. Chlorine Factory and Problem Statement

A chlorine factory equipped with an FC and hydrogen tank is considered in this study. The system structure of the chlorine factory is depicted in Fig. 1. Through electrolysis of brine, the EL generates chlorine, which is the main factory product. While producing chlorine, the EL generates hydrogen as a byproduct. The byproduct hydrogen is stored in a hydrogen tank as the energy resource of the FC. Electrical power mainly comes from the utility company. A part of the electricity comes from the FC. The remaining hydrogen stored in the tank is assumed to be sold to the hydrogen market.

The energy consumption of the EL accounts for the major proportion of the factory's energy consumption, as the factory's main production is dependent on the EL. Other factory loads, which account for minor proportions of the factory's energy consumption, refer to the energy consumption from auxiliary manufacturing processes, factory lighting, air conditioning, and other necessary electric facilities. An EMS is installed in the factory to monitor and control the main electric facilities in the factory through a local area network. The optimal power dispatch scheme, COPDA, is proposed and executed in the EMS to maximize factory profit. The optimal dispatch scheme of the FC output power induces a variation in the power purchased from the grid and the remaining byproduct hydrogen in the tank.

The day-ahead time-varying electricity prices are adopted along with the day-ahead constant sale price of hydrogen. To further improve economic profit, the factory participates in the incentive-based DR. The day-ahead electricity prices, DR requests, DR incentive rates, and DR time intervals are sent to the EMS through the Internet. The COPDA optimizes FC output power considering the time-varying electricity prices, DR incentive rates, and hydrogen sale prices. The amount of remaining hydrogen stored in the hydrogen tank is also optimized.

III. Modeling of Chlorine and Hydrogen Production

Let the sampling interval of COPDA be T_s (h). The total number of time steps for the COPDA being conducted every day is set as $J = 24/T_s$.

The main product, chlorine, is produced mainly in the EL. To ensure proper operation, the power consumption P_{el}^j of EL at every jth time step is bounded by an upper and lower bound, $P_{\text{el}}^{\max}$ and $P_{\text{el}}^{\min}$, respectively

$$P_{\text{el}}^{\min} \le P_{\text{el}}^j \le P_{\text{el}}^{\max}, j = 0, \ldots, (J-1). \tag{1}$$

The mass flow rate of chlorine production δ_{el}^j is a nonlinear function of P_{el}^j [13], [14]. In order to implement this nonlinear function into the proposed COPDA, a D_{el}-th-order polynomial is utilized to approximate this nonlinear function

$$\delta_{\text{el}}^j = \sum_{k=0}^{D_{el}} d_k (P_{\text{el}}^j)^k, j = 0, \ldots, (J-1) \tag{2}$$

where d_k is the kth-order coefficient of the polynomial in (2). The coefficient d_k is determined by applying curve fitting on the data provided by the EL manufacturing company and then fine-tuned by the chlorine production factory.

The mass flow rate σ_{el}^j of the hydrogen production at the jth time step is calculated as follows:

$$\sigma_{\text{el}}^j = \gamma_{\text{el}} \delta_{\text{el}}^j, j = 0, \ldots, (J-1) \tag{3}$$

where γ_{el} is the ratio of hydrogen generation to chlorine production.

Let P_{fc}^j and v_{fc}^j be the output power and power efficiency of the FC, respectively, at the jth time step. Hence, the mass flow

rate σ_{fc}^j of the FCs hydrogen consumption at the jth time step can be expressed as follows [23]:

$$\sigma_{\text{fc}}^j = \frac{P_{\text{fc}}^j}{\upsilon_{\text{fc}}^j \zeta}, j = 0, \ldots, (J-1) \tag{4}$$

where ζ is the lower heating value of hydrogen.

The power efficiency υ_{fc}^j is a nonlinear function of the partial load ratio $P_{\text{fc}}^j / P_{\text{fc}}^{\max}$ of FC, where $P_{\text{fc}}^{\max}$ is the FCs maximum power. In order to implement this nonlinear function into the proposed COPDA, a D_{fc}-th-order polynomial is utilized to approximate this nonlinear function [24]

$$\upsilon_{\text{fc}}^j = \sum_{k=0}^{D_{\text{fc}}} c_k \left(P_{\text{fc}}^j / P_{\text{fc}}^{\max}\right)^k, j = 0, \ldots, (J-1) \tag{5}$$

where c_k is the kth-order coefficient of the polynomial in (5). Similarly, the coefficient c_k is determined by applying curve fitting on the data provided by the FC manufacturing company and then fine-tuned by the FC user. Substituting (5) into (4), the FCs hydrogen consumption rate σ_{fc}^j is expressed as follows:

$$\sigma_{\text{fc}}^j = P_{\text{fc}}^j \Big/ \left(\zeta \sum_{k=0}^{D_{\text{fc}}} c_k \left(P_{\text{fc}}^j / P_{\text{fc}}^{\max}\right)^k\right), j = 0, \ldots, (J-1). \tag{6}$$

As depicted in Fig. 1, the hydrogen produced by the EL based on the mass flow rate, as in (3), is piped into the hydrogen tank. Similarly, the hydrogen consumed by FC is extracted from the hydrogen tank at the consumption rate calculated in (6). Denote Ω_h^j as the mass of the hydrogen in the tank at the jth time step. The hydrogen mass Ω_h^j dynamically changes due to hydrogen production, consumption, or both

$$\Omega_h^j = \Omega_h^{j-1} + \sigma_{\text{el}}^j T_s - \sigma_{\text{fc}}^j T_s, j = 0, \ldots, (J-1). \tag{7}$$

To ensure the reliability of the hydrogen tank, Ω_h^j is constrained between the lower and upper bound, $\Omega_h^{\min}$ and $\Omega_h^{\max}$, respectively

$$\Omega_h^{\min} \le \Omega_h^j \le \Omega_h^{\max}, j = 0, \ldots, (J-1). \tag{8}$$

The chlorine produced by the EL at every jth time step is piped into the chlorine storage. No chlorine is withdrawn from the chlorine storage for sale during the day, and chlorine accumulated in the storage is only sold to the customers at the day's end. The chlorine mass Ω_c^j in the chlorine storage at any jth time step is calculated as follows:

$$\Omega_c^j = \Omega_c^{j-1} + \delta_{\text{el}}^j T_s, j = 0, \ldots, (J-1). \tag{9}$$

The chlorine mass Ω_c^j is constrained between a lower and upper bound, $\Omega_c^{\min}$ and $\Omega_c^{\max}$, respectively, to ensure the reliability of the chlorine storage

$$\Omega_c^{\min} \le \Omega_c^j \le \Omega_c^{\max}, j = 0, \ldots, (J-1). \tag{10}$$

At the end of the day, Ω_c^j must be greater than the daily production target Ω_c^{target} in order to deliver customers with sufficient product quantity. Thus

$$\Omega_c^{J-1} \ge \Omega_c^{\text{target}} \tag{11}$$

where Ω_c^{J-1} is the chlorine mass calculated based on (9) at the end of the day, that is, the $(J-1)$th time step.

IV. Modeling of Electrical Power

The factory load P_L^j mainly comprises the EL load P_{el}^j and other auxiliary factory loads P_{aux}^j. Therefore

$$P_L^j = P_{\text{el}}^j + P_{\text{aux}}^j, j = 0, \ldots, (J-1). \tag{12}$$

The energy resource that satisfies the factory load P_L^j is mainly from the electrical power P_{grid}^j purchased from the power grid at every jth time step. In addition to P_{grid}^j, the electrical power P_{fc}^j generated from the FC is the other electric energy resource. The FC output power P_{fc}^j is optimized by COPDA. Thus, P_{grid}^j is determined through the power balance

$$P_{\text{grid}}^j = P_L^j - P_{\text{fc}}^j, j = 0, \ldots, (J-1). \tag{13}$$

Note that P_{grid}^j is constrained to be less than the contracted maximum power $P_{\text{grid}}^{\max}$ to avoid overload penalty. Similarly, P_{grid}^j is regulated to be greater than the minimum threshold $P_{\text{grid}}^{\min}$ for energy supply safety. Therefore

$$P_{\text{grid}}^{\min} \le P_{\text{grid}}^j \le P_{\text{grid}}^{\max}, j = 0, \ldots, (J-1). \tag{14}$$

It takes time to turn the FC ON and warm up the cell in order to get into the steady operation mode. The EMS controls the FC to remain running so that it can smoothly dispatch the generated power from the FC, considering the time-varying electricity prices. Therefore, FCs generated power P_{fc}^j is constrained by both upper and lower limits, $P_{\text{fc}}^{\max}$ and $P_{\text{fc}}^{\min}$, respectively, as follows:

$$P_{\text{fc}}^{\min} \le P_{\text{fc}}^j \le P_{\text{fc}}^{\max}, j = 0, \ldots, (J-1). \tag{15}$$

To avoid damage to the FC stack, the rate of power change is constrained by a factor $\kappa_{\text{fc}} \in [0, 1]$

$$\left|P_{\text{fc}}^{j+1} - P_{\text{fc}}^j\right| \le \kappa_{\text{fc}} \left(P_{\text{fc}}^{\max} - P_{\text{fc}}^{\min}\right), j = 0, \ldots, (J-1). \tag{16}$$

To further increase the factory's profit, assume that the factory participates in the incentive-based DR program by promising the utility company that the factory can curtail P_{grid}^j below the baseline load during the DR time interval. The EMS constantly regulates the power purchased from the grid P_{grid}^j to minimize the electricity cost and maximizes the payoff by curtailing P_{grid}^j for the incentive-based DR program. Denote τ_r^s and τ_r^e as the starting and ending points of the DR time interval, respectively. The factory's operator can choose any time interval within $[\tau_r^s, \tau_r^e]$ to curtail P_{grid}^j to be less than the baseline load. Let $\gamma^j \in \{0, 1\}$ be the factory operator's decision on the participation in DR at every jth time step within the interval $[\tau_r^s, \tau_r^e]$. The parameter $\gamma^j = 1$ if the factory operator chooses to participate in the incentive-based DR at the jth time step, and $\gamma^j = 0$; otherwise, $\forall j \in [\tau_r^s, \tau_r^e]$. If $\gamma^j = 1$, it means that the factory is willing to maintain the purchased power P_{grid}^j to be less than its baseline load $\bar{P}_{\text{base}}$. As the factory opts to participate in the DR, the COPDA curtails P_{grid}^j and yet increases P_{fc}^j to earn more DR incentives. The

baseline load $\bar{P}_{\text{base}}$ of the factory is the average load of the factory during the time interval of DR over the past M days

$$\bar{P}_{\text{base}} = \frac{1}{M} \cdot \frac{1}{\tau_r^e - \tau_r^s} \cdot \sum_{n=1}^{M} \sum_{j=\tau_r^s}^{\tau_r^e} P_{\text{grid},n}^j \tag{17}$$

where $P_{\text{grid},n}^j$ is the power purchased from the power grid at the jth time step on the past nth day. Note that $P_{\text{grid},n}^j$ is recorded in *the EMS*.

V. FC Optimal Power Dispatch

The COPDA is to optimally dispatch the FC output power P_{fc}^j by scheduling the hydrogen consumption. The optimization in COPDA is divided into four parts: maximizing the profit from selling the produced chlorine, maximizing the profit from selling the remaining byproduct hydrogen, minimizing the cost of purchased power under time-varying electricity prices, and maximizing the incentive payoffs for the incentive-based DR.

Let ρ_c be the chlorine price and B_c be the profit from selling the chlorine produced during the day

$$B_c = \rho_c \Omega_c^{J-1} \tag{18}$$

where Ω_c^{J-1} is the chlorine mass calculated based on (9) at the end of the day, that is, the $(J-1)$th time step.

Similarly, let ρ_h be the hydrogen price and B_h be the profit from selling the byproduct hydrogen accumulated at the end of the day. Thus

$$B_h = \rho_h \Omega_h^{J-1} \tag{19}$$

where Ω_h^{J-1} is the hydrogen mass calculated based on (7) at the end of the day.

Denote ρ_b^j and ρ_d^j as the day-ahead electricity price and incentive price, respectively, at every jth time step. Let the electricity cost at the jth time step be B_1^j, which is defined as follows:

$$B_1^j = \rho_b^j P_{\text{grid}}^j T_s, j = 0, \ldots, (J-1). \tag{20}$$

The incentive-based DR is designed to provide a payoff to the customer who joins the DR program and promises to curtail the purchased power from the grid during the DR interval to the level less than the contracted ratio $\chi(<1)$ of baseline load. In order to attract customers to join the incentive-based DR program, the incentive price ρ_d^j is usually much greater than the day-ahead price ρ_b^j. However, if the customer fails to curtail the purchased power P_{grid}^j below the contracted portion of baseline load $\bar{P}_{\text{base}}$ defined in (17), a penalty is charged based on the amount of power by which the P_{grid}^j exceeds the contracted portion of baseline load, i.e., $\chi\bar{P}_{\text{base}}$. Let B_2^j be the payoff the factory that can receive from the incentive-based DR program, which is defined as follows:

$$B_2^j = \begin{cases} \gamma^j \rho_d^j (\chi \bar{P}_{\text{base}} - P_{\text{grid}}^j), \text{if} P_{\text{grid}}^j \le \chi \bar{P}_{\text{base}} \\ \gamma^j f_1 \rho_d^j (\chi \bar{P}_{\text{base}} - P_{\text{grid}}^j), \text{if} \chi \bar{P}_{\text{base}} < P_{\text{grid}}^j \\ \qquad \le (1+\eta)\chi \bar{P}_{\text{base}} \\ \gamma^j f_2 \rho_d^j (\chi \bar{P}_{\text{base}} - P_{\text{grid}}^j), \text{if} (1+\eta)\chi \bar{P}_{\text{base}} < P_{\text{grid}}^j. \end{cases} \tag{21}$$

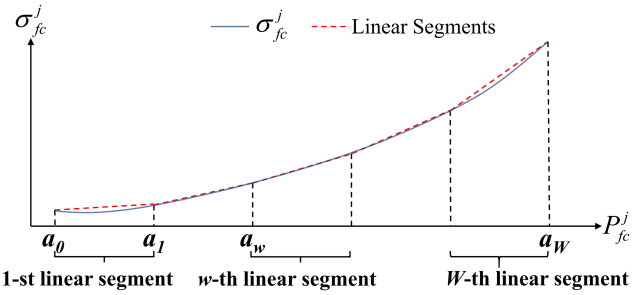

Fig. 2. Nonlinear relationship between hydrogen consumption rate and FC output power.

Here, $\eta > 0$ is the percentage by which P_{grid}^j can exceed $\chi\bar{P}_{\text{base}}$ for different penalty charges. The penalty charge rates f_1 and f_2, $f_2 > f_1 > 1$, are applied to different grades of penalty depending on the amount by which P_{grid}^j exceeds the contracted portion of baseline load, i.e., $\chi\bar{P}_{\text{base}}$. Referring to (21), the incentive payment B_2^j becomes negative, that is, becomes the penalty charge, if $P_{\text{grid}}^j > \chi\bar{P}_{\text{base}}$.

The optimization in COPDA is defined in terms of B_c, B_h, B_1^j, and B_2^j, as defined in (18), (19), (20), and (21), respectively. The FC output power P_{fc}^j at every jth time step is optimally dispatched to maximize the sale income B_c of the chlorine and remaining hydrogen B_h, minimize the electricity cost B_1^j, and maximize the incentive payment B_2^j from participating in DR. Therefore, the optimization conducted in COPDA is defined as follows:

$$\max_{P_{\text{el}}^j, P_{\text{fc}}^j, j=0,\ldots,J-1} \left(B_c + B_h - \sum_{j=0}^{J-1} B_1^j + \sum_{j=\tau_r^s}^{\tau_r^e} B_2^j \right) \tag{22}$$

which is subject to (1)–(3) and (6)–(17).

VI. Piecewise Linearization

The hydrogen consumption rate σ_{fc}^j defined in (6) is a nonlinear function of the optimization variable P_{fc}^j. The nonlinearity of σ_{fc}^j induces nonlinearity in the constraints in (7). Similarly, the chlorine production rate δ_{el}^j defined in (2) is a nonlinear function of the optimization variable P_{el}^j, which induces nonlinearity in the constraints in (3) and (9). Therefore, the optimization in (22) is a nonlinear problem. Although there have been various nonlinear optimization solvers, they are generally time-consuming and not necessarily convergent. In contrast, linear programming is computationally fast and easy to converge. A piecewise linearization scheme, along with the optimization, is proposed in this article so that the nonlinear optimization problem is turned into a linear problem and solved using linear programming. The nonlinear relationship between the hydrogen consumption rate σ_{fc}^j and the FC output power P_{fc}^j in (6) is depicted in Fig. 2. Fig. 2 shows that the nonlinear function is approximated by W consecutive linear segments.

Both terminal points of every linear segment can be either determined according to engineering experience or evenly assigned within the range $[P_{\text{fc}}^{\min}, P_{\text{fc}}^{\max}]$. Without the loss of generality, the terminal points are evenly assigned in this article. Let the terminal points be $a_w, w = 0, \ldots, W$, and they are evenly assigned as follows:

$$a_w = \begin{cases} P_{\text{fc}}^{\min}, w = 0 \\ a_{w-1} + \frac{P_{\text{fc}}^{\max} - P_{\text{fc}}^{\min}}{W}, w = 1, 2, \ldots, W. \end{cases} \tag{23}$$

Only one operation point exists in every optimization computation. In other words, only one linear segment is utilized to approximate the nonlinear function in (6). A binary auxiliary variable $z_w^j \in \{0, 1\}$ is introduced in the optimization such that $z_w^j = 1$ indicates that the operation point for optimization at the jth time step is located in the wth linear segment, and $z_w^j = 0$ otherwise. The constraint is set as follows to ensure that only one linear segment is selected to search for the optimal operation point:

$$\sum_{w=1}^{W} z_w^j = 1, j = 0, \ldots, (J-1). \tag{24}$$

A continuous auxiliary variable $\lambda_w^j \in [0, 1]$ is utilized to search for the optimal P_{fc}^j in the selected wth linear segment. Specifically, $\lambda_w^j = 0$ if the wth linear segment is not selected, and $\lambda_w^j \in [0, 1]$ if the wth linear segment is selected. The constraint for λ_w^j in association with z_w^j is set as follows:

$$0 \le \lambda_w^j \le z_w^j, w = 1, \ldots, W, j = 0, \ldots, (J-1). \tag{25}$$

Referring to (24) and (25), only one optimal linear segment is selected to search for the optimal P_{fc}^j.

Hence, P_{fc}^j in any wth linear segment is expressed as follows:

$$P_{\text{fc}}^j = \sum_{w=1}^{W} \left(a_{w-1} \cdot z_w^j + (a_w - a_{w-1}) \cdot \lambda_w^j\right). \tag{26}$$

The optimal P_{fc}^j in the linear segment with $z_w^j = 1$ is found by optimizing the corresponding λ_w^j.

The hydrogen consumption rate σ_{fc}^j in terms of P_{fc}^j in (6) is approximated by a piecewise linear function $\hat{\sigma}_{\text{fc}}^j$ as follows:

$$\hat{\sigma}_{\text{fc}}^j = \sum_{w=1}^{W} \left(z_w^j \sigma_{\text{fc}}^j(a_{w-1}) + \lambda_w^j \left(\sigma_{\text{fc}}^j(a_w) - \sigma_{\text{fc}}^j(a_{w-1})\right)\right) \tag{27}$$

where the nonlinear function $\sigma_{\text{fc}}^j(\cdot)$ is defined as in (6). The hydrogen consumption σ_{fc}^j in (7) is replaced with the approximated hydrogen consumption $\hat{\sigma}_{\text{fc}}^j$ in (27). A similar piecewise linearization in (23)–(27) is applied to the nonlinear relationship between chlorine production and the power consumption of the EL in (2), resulting in the following constraints:

$$b_u = \begin{cases} P_{\text{el}}^{\min}, u = 0 \\ b_{u-1} + \frac{P_{\text{el}}^{\max} - P_{\text{el}}^{\min}}{U}, u = 1, 2, \ldots, U \end{cases} \tag{28}$$

$$\sum_{u=1}^{U} y_u^j = 1, j = 0, \ldots, (J-1) \tag{29}$$

$$0 \le \mu_u^j \le y_u^j, u = 1, \ldots, U, j = 0, \ldots, (J-1) \tag{30}$$

$$P_{\text{el}}^j = \sum_{u=1}^{U} \left(b_{u-1} \cdot y_u^j + (b_u - b_{u-1}) \cdot \mu_u^j\right) \tag{31}$$

$$\hat{\delta}_{\text{el}}^j = \sum_{u=1}^{U} \left(y_u^j \delta_{\text{el}}^j(b_{u-1}) + \mu_u^j \left(\delta_{\text{el}}^j(b_u) - \delta_{\text{el}}^j(b_{u-1})\right)\right). \tag{32}$$

Here, U is the number of linear segments used to approximate the nonlinear relationship between chlorine production and the power consumption of EL, and b_u is the terminal point of the linear segments, $u = 0, \ldots, U$. The variable $y_u^j \in \{0, 1\}$ is binary such that $y_u^j = 1$ indicates that the optimal P_{el}^j is searched for in the uth linear segment. The variable $\mu_u^j \in [0, 1]$ is used to search for the best P_{el}^j in the selected uth linear segment. The chlorine production δ_{el}^j in (3) and (9) is replaced with the approximated chlorine production $\hat{\delta}_{\text{el}}^j$ in (32).

VII. Reformulation of Conditional Cost Function

The conditional cost function in (21) cannot be directly utilized as a part of the objective function in (22) for linear programming. A delicate mechanism is proposed to reformulate the conditional cost function. As shown in (14) and (21), P_{grid}^j can be located in any of the three different regions, $[P_{\text{grid}}^{\min}, \chi\bar{P}_{\text{base}}]$, $(\chi\bar{P}_{\text{base}}, (1+\eta)\chi\bar{P}_{\text{base}}]$, and $((1+\eta)\chi\bar{P}_{\text{base}}, P_{\text{grid}}^{\max}]$, which are, respectively, referred to as the first, second, and third regions for convenience. When P_{grid}^j is located in different regions, different cost functions are used to calculate the incentive payoffs. An auxiliary binary variable $\alpha_i^j \in \{0, 1\}, i = 1, \ldots, 3, j \in [\tau_r^s, \tau_r^e]$ is introduced to decide which region P_{grid}^j is located. The variable $\alpha_i^j = 1$ indicates that P_{grid}^j exists in the ith region. Note that P_{grid}^j is located only in one region; thus, the following constraint is set:

$$\sum_{i=1}^{3} \alpha_i^j = 1, j \in [\tau_r^s, \tau_r^e]. \tag{33}$$

A continuous auxiliary variable $\beta_i^j \in [0, 1]$ is introduced to decide the optimal point of P_{grid}^j that should be located in the ith region. The variable $\beta_i^j \in [0, 1]$ if $\alpha_i^j = 1$. Thus, the following constraint is set:

$$0 \le \beta_i^j \le \alpha_i^j, i = 1, \ldots, 3, j \in [\tau_r^s, \tau_r^e]. \tag{34}$$

Let $P_{\text{grid},i}^{\text{start}}$ and $P_{\text{grid},i}^{\text{end}}$ be the starting and ending points of the ith region, respectively. Subsequently, P_{grid}^j can be expressed as follows:

$$P_{\text{grid}}^j = \sum_{i=1}^{3} \alpha_i^j P_{\text{grid},i}^{\text{start}} + \beta_i^j \left(P_{\text{grid},i}^{\text{end}} - P_{\text{grid},i}^{\text{start}}\right), j \in [\tau_r^s, \tau_r^e]. \tag{35}$$

Let $B_{2,i}^{\text{start}}$ and $B_{2,i}^{\text{end}}$ be the incentive payoffs corresponding to the P_{grid}^j equal to $P_{\text{grid},i}^{\text{start}}$ and $P_{\text{grid},i}^{\text{end}}$, respectively. Note that the values of $B_{2,i}^{\text{start}}$ and $B_{2,i}^{\text{end}}$ are calculated based on (21). The incentive payoff B_2^j in terms of P_{grid}^j under different conditions

from (21) is reformulated as follows:

$$B_2^j = \sum_{i=1}^{3} \alpha_i^j B_{2,i}^{\text{start}} + \beta_i^j \left(B_{2,i}^{\text{end}} - B_{2,i}^{\text{start}}\right), j \in [\tau_r^s, \tau_r^s]. \quad (36)$$

Therefore, the conditional cost function in (21) is reformulated as in (36) with constraints in (33)–(35), which are suitable for linear programming.

The nonlinear optimization in (22) is transformed into a linear optimization problem by incorporating (23)–(36). The optimization in COPDA is reformulated as follows:

$$\max_{\substack{z_w^j,\lambda_w^j,w=1,\ldots,W,j=0,\ldots,J-1 \\ y_u^j,\mu_u^j,u=1,\ldots,U,j=0,\ldots,J-1 \\ \alpha_i^j,\beta_i^j,i=1,\ldots,3,j=\tau_r^s,\ldots,\tau_r^e}} \left(B_c + B_h - \sum_{j=0}^{J-1} B_1^j + \sum_{j=\tau_r^s}^{\tau_r^e} B_2^j \right) \quad (37)$$

subject to (1), (28)–(32), (3), (23)–(27), (7)–(17), and (33)–(36). The optimization is only conducted once at the beginning of a day and the optimization horizon is fixed to be totally J time steps. However, the EL load P_{el}^j and auxiliary factory loads P_{aux}^j are subject to uncertainties almost at every time step. It is vital to address these uncertainties in the optimization because the variations of both P_{el}^j and P_{aux}^j lead to different optimization results at every time step from the one optimized only once at the first time step. Therefore, the optimization in (37) is further modified to the real-time optimization. Essentially, the real-time optimization is designed to conduct the optimization at every current kth time step with the optimization horizon from the current kth time step to the end of the day, i.e., the $(J-1)$th time step, $k = 0, \ldots, (J-1)$. Although the optimal power dispatch is determined for the time interval $[k, J-1]$, only the optimal power dispatch decision at the kth time step is implemented. The real-time optimization modified from the day-ahead optimization in (37) is defined as (38) shown at the bottom of this page. Referring to (38), the term B_2^j is removed from the objective function as $k > \tau_r^e$ because the entire DR interval $[\tau_r^s, \tau_r^e]$ no longer falls into the optimization horizon $[k, J-1]$. On the other hand, the DR interval $[\tau_r^s, \tau_r^e]$ entirely falls into the optimization horizon $[k, J-1]$ as $k < \tau_r^s$. Therefore, the lower and upper bound for calculating B_2^j ranges from τ_r^s to τ_r^e, i.e., the entire DR interval, as $k < \tau_r^s$. However, if $\tau_r^s \le k \le \tau_r^e$, only a portion of the DR interval $[\tau_r^s, \tau_r^e]$ falls into the optimization horizon $[k, J-1]$. As a result, the calculation of the DR incentive payoffs B_2^j is started from the kth time step

TABLE II
PARAMETER SETTINGS

Parameter	Value	Parameter	Value
T_s	0.25 h	$c_k, k=0...D_{fc}$	0.903, 2.999, 3.650, -2.070, 0.462, 0.375
J	96	f_1 , f_2	1.5, 2.4
ζ	33.3 kWh/kg [27]	ρ_c	0.165 USD/kg [19]
$P_{el}^{\min}$, $P_{el}^{\max}$	1.028, 2.283 MW	ρ_h	1.697 USD/kg [19]
$P_{grid}^{\min}$, $P_{grid}^{\max}$	0, 4 MW	$\rho_d^j, j \in [\tau_r^s, \tau_r^e]$	0.2 USD/kWh
$\bar{P}_{base}$	2.28 MW	$\Omega_c^{\min}$, $\Omega_c^{\max}$	0, 36000 kg
$P_{fc}^{\min}$, $P_{fc}^{\max}$	0.3, 5 MW	$\Omega_h^{\min}$, $\Omega_h^{\max}$	0, 1080 kg
κ_{fc}	0.32	Ω_c^{target}	12000 kg
D_{el} , D_{fc}	2, 5	η	0.3
γ_{el}	0.03 [22]	Initial Ω_c^j	0 kg
τ_r^s, τ_r^e	10:00, 15:00	Initial Ω_h^j	0 kg
$d_k, k=0...D_{el}$	3×10^{-8} , 0.0005, 0.0278	χ	0.5

VIII. SIMULATIONS

Simulations were performed to evaluate the proposed optimization scheme in (38). The FC simulated in this section is a Proton Exchange Membrane FC. The optimization problem was solved using the CPLEX solver, and the simulations were performed in a workstation using AMD Ryzen 9 3900XT CPU @ 3.80 GHz.

A. Simulation Settings

Table II presents the parameter settings in the simulation. The coefficients $d_k, k = 0, \ldots, D_{\text{el}}$ are calculated by fitting the data generated using the EL model in [13]. The coefficients $c_k, k = 0, \ldots, D_{\text{fc}}$ are calculated by fitting the data generated using the FC model in [25] and [26].

B. Simulation Results

The electrical power dispatch results obtained by the COPDA are shown in Fig. 3. The factory's operator chose to participate in the incentive-based DR at certain time intervals within the DR time interval $[\tau_r^s, \tau_r^e]$. The gray areas in Fig. 3 indicate the

$$\begin{cases} \max\limits_{\substack{z_w^j,\lambda_w^j,w=1,\ldots,W,j=k,\ldots,J-1 \\ y_u^j,\mu_u^j,u=1,\ldots,U,j=k,\ldots,J-1 \\ \alpha_i^j,\beta_i^j,i=1,\ldots,3,j=\tau_r^s,\ldots,\tau_r^e}} \left(B_c + B_h - \sum_{j=k}^{J-1} B_1^j + \sum_{j=\tau_r^s}^{\tau_r^e} B_2^j\right), & \text{if} k < \tau_r^s \\ \max\limits_{\substack{z_w^j,\lambda_w^j,w=1,\ldots,W,j=k,\ldots,J-1 \\ y_u^j,\mu_u^j,u=1,\ldots,U,j=k,\ldots,J-1 \\ \alpha_i^j,\beta_i^j,i=1,\ldots,3,j=k,\ldots,\tau_r^e}} \left(B_c + B_h - \sum_{j=k}^{J-1} B_1^j + \sum_{j=k}^{\tau_r^e} B_2^j\right), & \text{if} \tau_r^s \le k \le \tau_r^e \\ \max\limits_{\substack{z_w^j,\lambda_w^j,w=1,\ldots,W,j=k,\ldots,J-1 \\ y_u^j,\mu_u^j,u=1,\ldots,U,j=k,\ldots,J-1}} \left(B_c + B_h - \sum_{j=k}^{J-1} B_1^j\right), & \text{if} k > \tau_r^e. \end{cases} \quad (38)$$

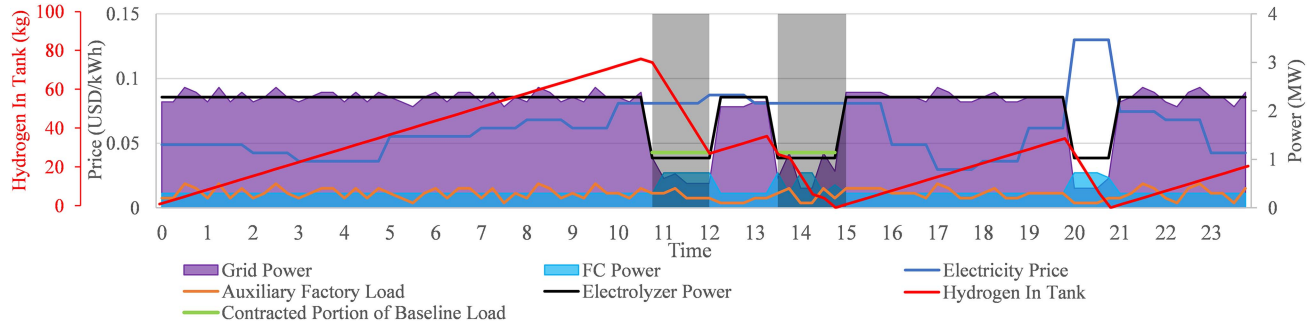

Fig. 3. Electrical power dispatch results obtained by the COPDA.

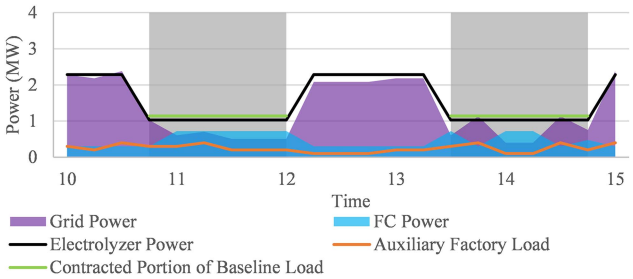

Fig. 4. Electrical power dispatch results during DR time intervals for the chlorine price of 0.165 USD/kg.

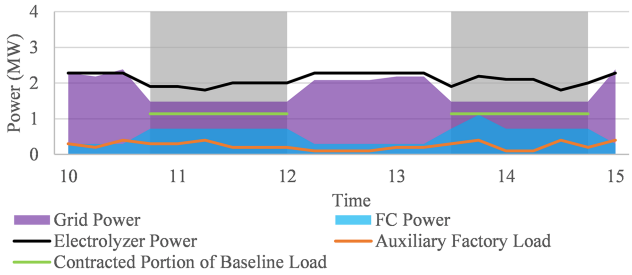

Fig. 5. Electrical power dispatch results during DR time intervals for the chlorine price of 1.3 USD/kg.

time intervals when the factory's operator chose to participate in the incentive-based DR. The EMS purchases a large amount of electricity from 00:00 to 10:00 to avoid consuming a large amount of hydrogen. This is to accumulate the byproduct hydrogen in the hydrogen tank so that there is enough hydrogen for use at 10:45–12:15 and 13:30–15:00, thereby reducing the need to purchase electricity during this interval. Note that the electricity prices at 10:45–12:15 and 13:30–15:00 are relatively high. The factory's operator chose to participate in the incentive-based DR at 10:45–12:15 and 13:30–15:00. As the EMS tries to avoid purchasing electricity at 10:45–12:15 and 13:30–15:00, the factory's energy consumption during this period is primarily supplemented by the FCs power. Although the FC consumed some hydrogen to generate enough electrical power, the COPDA managed to generate enough hydrogen for sale. Fig. 3 shows that hydrogen accumulation began around 21:00 to have more hydrogen for sale at the end of the day so that the revenue from selling hydrogen can be maximized.

The electrical power dispatch results during the incentive-based DR time intervals when the chlorine prices of 0.165 and 1.3 USD/kg are used for simulations are shown in Fig. 4 and Fig. 5, respectively. The gray areas in Figs. 4 and 5 indicate the time intervals when the factory's operator chose to participate in the incentive-based DR. When the price of chlorine is 0.165 USD/kg, the power purchase is kept below the contracted portion of baseline load during the incentive-based DR time intervals to prevent being penalized by the utility. However, when the price of chlorine is 1.3 USD/kg, P^{j}_{grid} is above the contracted portion of the baseline load to produce more chlorine for sale. This is because the chlorine price is so high that even if a penalty is charged by the utility, producing more chlorine for sale will still be the best decision.

TABLE III
TOTAL FC-GENERATED ENERGY AND THE FACTORY'S TOTAL PROFIT WITH DIFFERENT HYDROGEN PRICES

Hydrogen Price (USD/kg)	Total FC Energy Output (MWh)	Total Profit (USD)
0.339	8.8	1136.70
1.697	8.49	1155.14
8.5	7.2	1839.63

Table III presents the total FC-generated energy and the factory's total profit when different hydrogen prices are used for simulations. The total FC-generated energy output decreases as the hydrogen price increases. This is because when hydrogen prices are relatively high, high profits can be generated from selling hydrogen. Therefore, an increase in the price of hydrogen greatly reduces the FC-generated energy to accumulate more hydrogen for sale.

The incentive payoffs from the DR program and the total profit of the factory under different chlorine prices are compared in Table IV. When the chlorine price rises to 1.3 and 2.4 USD/kg, COPDA tends to keep producing chlorine during the DR interval without decreasing the power consumption of EL in order to maximize the total profit. This results in the factory being charged a penalty for its failure to curtail its electricity purchases below the contracted portion of the baseline load during the DR interval. Despite being charged with a penalty, the total profit of the factory remains substantial because the chlorine price is

TABLE IV
DR INCENTIVE PAYOFFS AND THE FACTORY'S TOTAL PROFIT WITH DIFFERENT CHLORINE PRICES

Chlorine Price (USD/kg)	Incentive Payoffs (USD)	Total Profit (USD)
0.165	270.81	1155.14
1.3	−307.8 (Penalty)	27 366.70
2.4	−740.63 (Penalty)	53 720.70

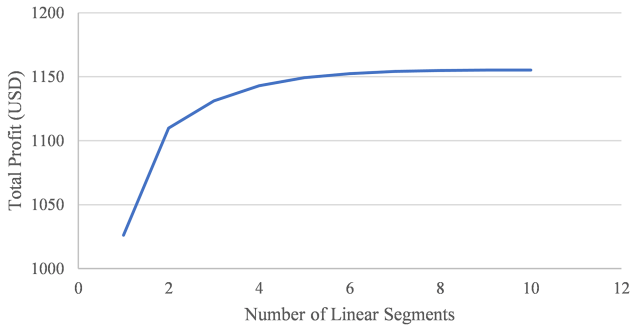

Fig. 6. Total profit versus the number of linear segments used to linearize the FCs nonlinear relationship.

high enough so that it is able to offset the incurred penalties and contribute to an overall rise in the factory's total profit.

C. Verification of the Piecewise Linearization Models

To optimize the power dispatch of chlorine factory accurately, the proposed COPDA considers the nonlinear relationship between the FC output power and hydrogen consumption as well as that between the EL power consumption and chlorine production. The inclusion of the nonlinear relationships results in the proposed COPDA being unable to be solved by MILP. This is because nonlinear cost functions and constraints are not compatible with MILP. Piecewise linearization models were adopted along with delicately designed constraints to formulate an MILP-compatible form of the nonlinear relationship between FC output power and hydrogen consumption as well as that between EL power consumption and chlorine production, as shown in (23)–(27) and (28)–(32), respectively. However, the correctness of the piecewise linearization models in (23)–(27) and (28)–(32) cannot be evaluated intuitively due to their complexities. Extensive experiments were designed and conducted to evaluate the correctness of the piecewise linearization models in (23)–(27) and (28)–(32). The experiment involved solving the proposed COPDA by using a varying number of linear segments in the piecewise linearization models for FC and EL and observing the resulting objective function value. Fig. 6 shows the variations in the total profit (i.e., objective function value) versus the number of linear segments used in the piecewise linearization model for the FC. It is observed that the total profit converges around six pieces. Therefore, the accuracy of the piecewise linearization model for FC is justified, which justifies the accuracy of the piecewise linearization model in an optimization scheme [28], [29]. In addition, the piecewise linearization model for EL is validated using the same experiment as well.

TABLE V
COMPARISON IN DIFFERENT INCENTIVE-BASED DR PROGRAMS

Incentive-Based DR program	Incentive Price (USD/kWh)	DR interval (time)	Incentive Payoffs (USD)	Total Profit (USD)
A	0.02	10:00–12:45	4.36	939.61
B	0.02	10:00–15:00	9.21	934.63
C	0.20	10:00–12:45	227.69	1124.04
D	0.20	10:00–15:00	270.81	1155.14

D. Comparison of Different Incentive-Based DR Programs

The proposed COPDA has been solved under different incentive-based DR programs, each distinguished by unique incentive prices and distinct DR intervals. It is assumed that the factory's chosen time intervals for participating in incentive-based DR are predetermined, which are 10:45–12:15 and 13:30–15:00, and remain unchanged across the different incentive-based programs. The profit obtained from participating in different incentive-based DR programs is compared in Table V. In Table V, the factory received a higher incentive payoff from program B compared with that from program A. This is attributed to the factory's prolonged engagement in program B than in program A. Although the factory receives a higher incentive payoff in program B, its total profit in program B is lower than that in program A. This is because the COPDA reduced chlorine production and utilized the byproduct hydrogen for electricity generation to allow the factory to participate in incentive-based DR for an extended period. As a result, the factory's profit from chlorine and byproduct hydrogen sales is reduced in program B, resulting in a lower total profit compared with program A.

Comparing program C with program D, it is observed that the total profit of the factory in program D is higher than that in program C, despite the factory's prolonged participation in the incentive-based DR in program D. This is because the incentive price is high enough so that even the factory reduces its chlorine and byproduct hydrogen sale for prolonged DR participation in program D; the total profit in program D is still higher than in program C.

IX. CONCLUSION

In this article, an optimal power dispatch scheme was proposed for a chlorine factory with FCs that participate in incentive-based DR. Although the proposed optimization was intended for chlorine factories, with minor modifications, the proposed COPDA can also be applied to a factory that generates byproduct hydrogen during production and utilizes the hydrogen as the energy resource of FC. The hydrogen generated from the manufacturing or production process is called "gray hydrogen," and it is becoming increasingly important in the energy market. The proposed COPDA assumed that the hydrogen remaining in the tank at the end of the day was sold to a retailer at a fixed price. As the concept of DR becomes increasingly prevalent, time-varying hydrogen prices could be adopted in the energy market. The proposed scheme can be modified to enable hydrogen sales at every time step considering time-varying hydrogen prices.

REFERENCES

[1] Y. Cao, W. Wei, L. Chen, Q. Wu, and S. Mei, "Supply inadequacy risk evaluation of stand-alone renewable powered heat-electricity energy systems: A data-driven robust approach," *IEEE Trans. Ind. Inform.*, vol. 17, no. 3, pp. 1937–1947, Mar. 2021.

[2] M. Pourakbari-Kasmaei, M. Lehtonen, J. Contreras, and J. R. S. Mantovani, "Carbon footprint management: A pathway toward smart emission abatement," *IEEE Trans. Ind. Inform.*, vol. 16, no. 2, pp. 935–948, Feb. 2020.

[3] G. Liu et al., "Real-time corporate carbon footprint estimation methodology based on appliance identification," *IEEE Trans. Ind. Inform.*, vol. 19, no. 2, pp. 1401–1412, Feb. 2023, doi: 10.1109/TII.2022.3154467.

[4] D. Li, W.-Y. Chiu, H. Sun, and H. V. Poor, "Multiobjective optimization for demand side management program in smart grid," *IEEE Trans. Ind. Inform.*, vol. 14, no. 4, pp. 1482–1490, Apr. 2018.

[5] F. Yao, Z. Y. Dong, K. Meng, Z. Xu, H. H.-C. Iu, and K. P. Wong, "Quantum-inspired particle swarm optimization for power system operations considering wind power uncertainty and carbon tax in Australia," *IEEE Trans. Ind. Inform.*, vol. 8, no. 4, pp. 880–888, Nov. 2012.

[6] Y. Zhang, H. H.-C. Iu, T. Fernando, F. Yao, and K. Emami, "Cooperative dispatch of BESS and wind power generation considering carbon emission limitation in Australia," *IEEE Trans. Ind. Inform.*, vol. 11, no. 6, pp. 1313–1323, Dec. 2015.

[7] E. Worrell, D. Phylipsen, D. Einstein, and N. Martin, "Energy use and energy intensity of the U.S. chemical industry," Lawrence Berkeley Nat. Lab., Univ. California, Berkeley, CA, USA, Tech. Rep. LBNL-44314, 2000.

[8] A. J. L. Verhage, J. F. Coolegem, M. J. J. Mulder, M. H. Yildirim, and F. A. de Bruijn, "30000 h operation of a 70 kW stationary PEM fuel cell system using hydrogen from a chlorine factory," *Int. J. Hydrogen Energy*, vol. 38, no. 11, pp. 4714–4724, Apr. 2013.

[9] C. A. Babu and S. Ashok, "Peak load management in electrolytic process industries," *IEEE Trans. Power Syst.*, vol. 23, no. 2, pp. 399–405, May 2008.

[10] J. I. Otashu and M. Baldea, "Demand response-oriented dynamic modeling and operational optimization of membrane-based Chlor-Alkali plants," *Comput. Chem. Eng.*, vol. 121, pp. 396–408, Nov. 2019.

[11] J. M. Simkoff and M. Baldea, "Stochastic scheduling and control using data-driven nonlinear dynamic models: Application to demand response operation of a chlor-alkali plant," *Ind. Eng. Chem. Res.*, vol. 59, no. 21, pp. 10031–10042, May 2020.

[12] J. Baetens, J. D. M. De Kooning, G. van Eetvelde, and L. Vandevelde, "A two-stage stochastic optimisation methodology for the operation of a chlor-alkali electrolyser under variable DAM and FCR market prices," *Energies*, vol. 13, no. 21, 2020, Art. no. 5675.

[13] K. Roh, L. C. Brée, K. Perrey, A. Bulan, and A. Mitsos, "Flexible operation of switchable Chlor-Alkali electrolysis for demand side management," *Appl. Energy*, vol. 255, 2019, Art. no. 113880.

[14] K. Roh, L. C. Brée, K. Perrey, A. Bulan, and A. Mitsos, "Optimal oversizing and operation of the switchable chlor-alkali electrolyzer for demand side management," *Comput. Aided Chem. Eng.*, vol. 46, pp. 1771–1776, 2019.

[15] X. Wang, H. Teichgraeber, A. Palazoglu, and N. H. El-Farra, "An economic receding horizon optimization approach for energy management in the chlor-alkali process with hybrid renewable energy generation," *J. Process Control*, vol. 24, no. 8, pp. 1318–1327, 2014.

[16] X. Wang, C. Tong, A. Palazoglu, and N. H. El-Farra, "Energy management for the chlor-alkali process with hybrid renewable energy generation using receding horizon optimization," in *Proc. IEEE 53rd Conf. Decis. Control*, Los Angeles, CA, USA, 2014, pp. 4838–4843.

[17] M. G. Rasul, M. A. Hazrat, M. A. Sattar, M. I. Jahirul, and M. J. Shearer, "The future of hydrogen: Challenges on production, storage and applications," *Energy Convers. Manage.*, vol. 272, 2022, Art. no. 116326.

[18] S. Bosu and N. Rajamohan, "Recent advancements in hydrogen storage—Comparative review on methods, operating conditions and challenges," *Int. J. Hydrogen Energy*, to be published, doi: 10.1016/j.ijhydene.2023.01.344.

[19] H. Teichgraeber and A. R. Brandt, "Optimal design of an electricity-intensive industrial facility subject to electricity price uncertainty: Stochastic optimization and scenario reduction," *Chem. Eng. Res. Des.*, vol. 163, pp. 204–216, 2020.

[20] Y. Huang, W. Wang, and B. Hou, "A hybrid algorithm for mixed integer nonlinear programming in residential energy management," *J. Cleaner Prod.*, vol. 226, pp. 940–948, Jul. 2019.

[21] Y. Huang, J. Zhang, Y. Mo, S. Lu, and J. Ma, "A hybrid optimization approach for residential energy management," *IEEE Access*, vol. 8, pp. 225201–225209, 2020.

[22] E. Chlor, "Questions and answers on the Chlor-Alkali sector and the EU emission trading system (ETS)," Brussels, Belgium, May 2010. Accessed: Oct. 26, 2022. [Online]. Available: https://www.eurochlor.org/wp-content/uploads/2019/04/3-2-questions_and_answers_on_the_chlor-alkali_sector_and_the_eu_emission_trading_system.pdf

[23] S. Nojavan and K. Zare, "Optimal energy pricing for consumers by electricity retailer," *Int. J. Elect. Power Energy Syst.*, vol. 102, pp. 401–412, Nov. 2018.

[24] M. Rouholamini and M. Mohammadian, "Energy management of a grid-tied residential-scale hybrid renewable generation system incorporating fuel cell and electrolyzer," *Energy Build*, vol. 102, pp. 406–416, Sep. 2015.

[25] L. Yao and J. C. Teo, "Optimization of power dispatch with load scheduling for domestic fuel cell-based combined heat and power system," *IEEE Access*, vol. 10, pp. 5968–5979, 2022.

[26] L. Yao and J. C. Teo, "Home energy management system of fuel cell-based CHP system with electric and thermal load scheduling," in *Proc. IEEE Int. Conf. Environ. Elect. Eng. IEEE Ind. Commercial Power Syst. Eur.*, 2021, pp. 1–6.

[27] V. Khaligh, A. Ghezelbash, M. Mazidi, J. Liu, J.-H. Ryu, and J. Na, "A stochastic agent-based cooperative scheduling model of a multi-vector microgrid including electricity, hydrogen, and gas sectors," *J. Power Sources*, vol. 546, 2022, Art. no. 231989.

[28] A. Safdarian, M. Fotuhi-Firuzabad, and M. Lehtonen, "Integration of price-based demand response in DisCos' short-term decision model," *IEEE Trans. Smart Grid*, vol. 5, no. 5, pp. 2235–2245, Sep. 2014.

[29] M. MansourLakouraj, M. Shahabi, M. Shafie-Khah, and J. P. S. Catalão, "Optimal market-based operation of microgrid with the integration of wind turbines, energy storage system and demand response resources," *Energy*, vol. 239, Jan. 2022, Art. no. 122156.

Leehter Yao (Senior Member, IEEE) received the Diploma degree from the National Taipei Institute of Technology, Taipei, Taiwan, in 1982, the M.S. degree from the University of Missouri, Rolla, MO, USA, in 1987, and the Ph.D. degree from the University of Wisconsin-Madison, Madison, WI, USA, in 1992, all in electrical engineering.

Since 1992, he has been with the Department of Electrical Engineering, National Taipei University of Technology, Taipei, where he is currently a Chair Professor. He has held over 30 patents mostly in the areas of power system monitoring and control and industrial applications of computational intelligence. His current research interests include intelligent control, demand response, and computational intelligence.

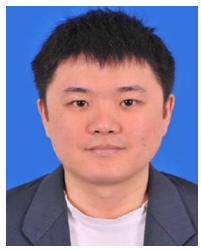

Jin Chuan Teo received the B.Eng. degree with first-class honors and the Doctor of Philosophy degree from UCSI University, Kuala Lumpur, Malaysia, in 2014 and 2020, respectively, both in electrical and electronic engineering.

These degrees emphasize his dedicated focus on electrical and electronic engineering. He is currently a Postdoctoral Researcher with the Department of Electrical Engineering, National Taipei University of Technology, Taipei, Taiwan. His primary areas of interest are centered around energy management systems for residential household, communities, and fuel cell systems. In addition, his work extends to researching distributed optimization algorithms for community energy management systems.